Protein Science (1992), *1*, 1112–1122. Cambridge University Press. Printed in the USA.

Control of phosphorylase *b* conformation by a modified cofactor: Crystallographic studies on R-state glycogen phosphorylase reconstituted with pyridoxal 5′-diphosphate

D.D. LEONIDAS,[1] N.G. OIKONOMAKOS,[1] A.C. PAPAGEORGIOU,[1]
K.R. ACHARYA,[2] D. BARFORD,[3,4] AND L.N. JOHNSON[3]

[1] Institute of Biological Research and Biotechnology, National Hellenic Research Foundation, Athens 11635, Greece
[2] Department of Biochemistry, University of Bath, Claverton Down, Bath BA2 7AY, United Kingdom
[3] Laboratory of Molecular Biophysics, University of Oxford, The Rex Richards Building, South Parks Road Oxford OX1 3QU, United Kingdom

(RECEIVED January 7, 1992; REVISED MANUSCRIPT RECEIVED March 25, 1992)

Abstract

Previous crystallographic studies on glycogen phosphorylase have described the different conformational states of the protein (T and R) that represent the allosteric transition and have shown how the properties of the 5′-phosphate group of the cofactor pyridoxal phosphate are influenced by these conformational states. The present work reports a study on glycogen phosphorylase *b* (GP*b*) complexed with a modified cofactor, pyridoxal 5'-diphosphate (PLPP), in place of the natural cofactor. Solution studies (Withers, S.G., Madsen, N.B., & Sykes, B.D., 1982, *Biochemistry 21*, 6716–6722) have shown that PLPP promotes R-state properties of the enzyme indicating that the cofactor can influence the conformational state of the protein. GP*b* complexed with pyridoxal 5′-diphosphate (PLPP) has been crystallized in the presence of IMP and ammonium sulfate in the monoclinic R-state crystal form and the structure refined from X-ray data to 2.8 Å resolution to a crystallographic *R* value of 0.21. The global tertiary and quaternary structure in the vicinity of the Ser 14 and the IMP sites are nearly identical to those observed for the R-state GP*b*–AMP complex. At the catalytic site the second phosphate of PLPP is accommodated with essentially no change in structure from the R-state structure and is involved in interactions with the side chains of two lysine residues (Lys 568 and Lys 574) and the main chain nitrogen of Arg 569. Superposition of the T-state structure shows that were the PLPP to be incorporated into the T-state structure there would be a close contact with the 280s loop (residues 282–285) that would encourage the T to R allosteric transition. The second phosphate of the PLPP occupies a site that is distinct from other dianionic binding sites that have been observed for glucose-1-phosphate and sulfate (in the R state) and for heptulose-2-phosphate (in the T state). The results indicate mobility in the dianion recognition site, and the precise position is dependent on other linkages to the dianion. In the modified cofactor the second phosphate site is constrained by the covalent link to the first phosphate of PLPP. The observed position in the crystal suggests that it is too far from the substrate site to represent a site for catalysis.

Keywords: allosteric control; glycogen phosphorylase; pyridoxal diphosphate; pyridoxal phosphate

Glycogen phosphorylase catalyzes the first step in the intracellular breakdown of glycogen in muscle in a reaction that is dependent on the cofactor pyridoxal phosphate. The response of the cofactor and the control properties of the enzyme are closely related. This paper reports a study on glycogen phosphorylase reconstituted with a modified cofactor that promotes the R state in order to further elaborate the relationships between conformational state and the cofactor.

Phosphorylase is controlled by shifts in the equilibrium between inactive (T-state) and active (R-state) conformations promoted by binding of allosteric effectors and reversible phosphorylation at Ser 14 . The dephosphorylated form, GP*b*, is dependent on AMP or IMP for ac-

Reprint requests to: Louise N. Johnson, Laboratory of Molecular Biophysics, University of Oxford, The Rex Richards Building, South Parks Road, Oxford OX1 3QU, United Kingdom.
[4] Present address: Cold Spring Harbor Laboratory, P.O. Box 100, Cold Spring Harbor, New York 11724.

Abbreviations: GP*b* and GP*a*, glycogen phosphorylase *b* and *a*; 1,4-α-D-glucan, orthophosphate α-glucosyltransferase (EC 2.4.1.1); glucose-1-P, α-D-glucose-1-phosphate; PLP, pyridoxal 5′-phosphate; PLPP, pyridoxal 5′-diphosphate.

tivity and is inhibited by glucose-6-phosphate and ATP. The phosphorylated form, GP*a*, is active in the absence of AMP, but activity is increased (by about 20%) in the presence of AMP. The properties of the enzyme have been reviewed (Graves & Wang, 1972; Madsen, 1986; Sprang et al., 1988; Johnson et al., 1989; Oikonomakos et al., 1991). The effects of serine phosphorylation can be mimicked by high concentrations of sulfate. Sulfate binds at the Ser-P site and favors the active R-state conformation (Barford & Johnson, 1989; Leonidas et al., 1991). On activation, glycogen phosphorylase utilizes inorganic phosphate to promote the phosphorylation of the α-1,4-glycosidic linkage in glycogen or oligosaccharide substrates to release glucose-1-P. Crystal structures of the four conformational states of the enzyme (T-state GP*b* [Acharya et al., 1991], T-state GP*a* [Sprang et al., 1988], R-state GP*b* [Barford & Johnson, 1989; Sprang et al., 1991], and R-state GP*a* [Barford et al., 1991], are available, and these have provided a structural explanation of the allosteric and catalytic properties of the enzyme.

The essential cofactor, PLP (Baranowski et al., 1957), is linked through a Schiff base to Lys 680 (Fischer et al., 1958; Titani et al., 1977). Removal of the cofactor results in inactivation, but the apoenzyme can be fully reactivated by reconstitution with PLP (Hedrick et al., 1966; Shaltiel et al., 1969). Reconstitution experiments with a number of modified cofactors (see Madsen & Withers, 1986; Johnson et al., 1989; Palm et al., 1990, for reviews) have demonstrated that the 5′-phosphate plays an obligatory role in catalysis. Only PLP analogues with a dianion that can be protonated (such as $-OPO_3^{2-}$ or $-CH_2PO_3^{2-}$) give significant activity. The enzyme reconstituted with pyridoxal is inactive, but addition of dianions (such as phosphite) can confer activity. The activity is inhibited by pyrophosphate, which is competitive with both the dianion and the substrate phosphate, and this observation provided the first direct evidence for the proximity of the substrate and cofactor phosphates (Parrish et al., 1977). ^{31}P-NMR studies showed that the state of ionization of the cofactor is dependent on the state of activation of the enzyme: the 5′-phosphate is a monoanion in the T-state conformation and a dianion in the R-state conformation. In the presence of substrates or inhibitors there is a change in the ^{31}P chemical shift, which has been interpreted either as a partially protonated state or as a distorted dianion (Feldman & Hull, 1977; Helmreich & Klein, 1980; Withers et al., 1981b).

There have been two main proposals for the role of the 5′-phosphate in the catalytic mechanism based on crystallographic, biochemical, and NMR studies (reviewed in Madsen & Withers, 1986; Johnson et al., 1989; Palm et al., 1990). Both mechanisms invoke close interactions between the cofactor 5′-phosphate and the substrate phosphate. In one proposal it is suggested that the 5′-phosphate group functions in an acid–base mechanism to promote attack by the substrate phosphate on the polysaccharide substrate. In the other proposal a closer association of the cofactor and substrate phosphates is envisaged in which the 5′-phosphate group acts as an electrophile to promote the attack by the substrate phosphate. Both proposals depend on the correct orientation of the substrate phosphate with respect to the cofactor phosphate. The interacting phosphate hypothesis was directly demonstrated in the crystallographic and NMR analysis of the complex of GP*b* with the product, heptulose-2-phosphate (McLaughlin et al., 1984; Klein et al., 1986; Johnson et al., 1990). In this complex the cofactor phosphorus to product phosphorus separation is 4.8 Å, and there is a hydrogen bond between the two phosphate groups. The noncovalent proximity of the product phosphate to the cofactor phosphate provided support for the mechanism in which the cofactor phosphate promotes attack by inorganic phosphate on the substrate by the general acid mechanism (Johnson et al., 1990; Palm et al., 1990).

The modified cofactor PLPP (Shimomura & Fukui, 1978) provides a covalent link between the two phosphates similar to that envisaged in the electrophilic mechanism. Phosphorylase reconstituted with PLPP is not active, but the modified enzyme exhibits properties of the R-state conformation as detected by high affinity for AMP and aggregation of dimers to tetramers (Withers et al., 1982). Thus, to paraphrase Perutz (1970) not only does the protein control the cofactor but the cofactor can control the protein. The crystal structure of PLPP-reconstituted GP*b* has been studied at 2.8 Å resolution with crystals grown in the presence of ammonium sulfate in order to define the structure of the modified cofactor in phosphorylase and to elucidate the relationship of the diphosphate binding site to those of the cofactor monophosphate binding site, the substrate phosphate sites, and their role in catalysis. Recently, the structure of R-state GP*b* with the modified cofactor PLPP has been solved from crystals grown in the presence of polyethyleneglycol (Sprang et al., 1991), and the environment of the PLPP in this structure is described in the accompanying paper (Sprang et al., 1992).

Results

Previous studies had defined a tetragonal crystal form of GP*b*, which is obtained in the presence of low salt and 10 mM magnesium acetate and in which the enzyme is in the T state, and a monoclinic crystal form obtained in the presence of 1 M ammonium sulfate in which the sulfate ions activate by binding at the Ser-P site in addition to binding at the AMP and the catalytic sites. In the R-state crystals the enzyme is a tetramer, a characteristic oligomerization state for activated R-state phosphorylase in the absence of glycogen.

Monoclinic R-state crystals of GP*b* reconstituted with PLPP in place of the natural cofactor grew either with

1.0–1.2 M ammonium sulfate or in the presence of 6 mM IMP and 1.2–1.4 M ammonium sulfate. Inclusion of IMP in the crystallization medium gave larger crystals within a few days. Cocrystallization in the presence of AMP was not attempted. A previous study had shown that cocrystallization of the native GP*b* with AMP resulted in doubling of the c unit cell edge (D. Leonidas & N.G. Oikonomakos, unpubl.). This change has also been observed on diffusion of ligands (e.g., glucose-1-P) into preformed R-state crystals, and here detailed X-ray analysis showed there were essentially no changes in conformation of the enzyme despite the increase in unit cell length (S.-H. Hu & D. Barford, unpubl.). Limited quantities of PLPP prevented crystallization trials under T-state conditions. However, previous experiments (Oikonomakos et al., 1987) had shown that GP*b* complexed with other cofactors that result in a shift of the enzyme toward the R state, such as pyridoxal, pyridoxal plus pyrophosphate, and PLP monomethyl ester, failed to crystallize under T-state conditions, and hence it might be anticipated that phosphorylase reconstituted with PLPP would also fail to crystallize in the T-state form. Kinetic analysis has shown that sulfate-activated GP*b* (enzyme-glycogen-lucose-1-P complex) exhibits a high affinity for AMP (K_α = 3.1 μM) and V_{max} = 70 μmol/min/mg at 0.9 M ammonium sulfate (Leonidas et al., 1990). The corresponding values for IMP are K_α = 120 μM and V_{max} = 56 μmol/min/mg under similar conditions.

A summary of the crystallographic data collection, data processing, and refinement statistics is given in Table 1. Tetrameric R-state GP*b* has 222 symmetry with approximately equivalent subunits that differ in Cα positions from the mean structure by a root mean square (rms) distance of 0.3 Å, a value that indicates the subunits are identical in their overall conformation to within the limits of the 2.8-Å resolution data. The precision of the refined structure of the R-state PLPP-GP*b*-IMP was similar to that described for the native structures of R-state GP*a* and R-state GP*b* (Barford & Johnson, 1989; Barford et al., 1991) as judged from the refinement parameters and Ramachandran and *B*-factor plots. The estimated error in coordinates from a Luzzati plot is between 0.2 and 0.3 Å. Examination of the electron density maps calculated after refinement based on coefficients $2F_o - F_c$ and calculated phases and of the map averaged over the four subunits showed that refinement had proceeded satisfactorily (Fig. 1A). There was an indication in the unaveraged map for a correction in the side chain position for Arg 569 in subunit 2. The electron density showed this side chain had shifted so that it contacted the second phosphate of PLPP. In subunit 1 in the unaveraged map there was weak indication for some conformational heterogeneity of this residue but no indication for shifts in subunits 3 and 4. The temperature factors for the terminal atoms of the Arg 569 side chain were higher in all four subunits than those observed in the native R-state

Table 1. *Crystal parameters, data collection, data processing, and refinement statistics of R-state GPb and the R-state PLPP-GPb-IMP complex*

	Space group	a (Å)	b (Å)	c (Å)	β (°)
A. Crystal parameters					
R-state GP*b*[a]	$P2_1$	119.0	190.0	88.2	109.35
R-state PLPP-GP*b*-IMP	$P2_1$	119.0	188.1	88.1	109.29

	No. of crystals	No. of measurements	No. of unique reflections	R_m[b]	% Complete (resolution)
B. Data processing statistics					
R-state GP*b*[a]	11	131,558	64,860	0.130	88 (2.8 Å)
R-state PLPP-GP*b*-IMP	6	107,286	78,049	0.108	98 (2.8 Å)

	Reflections $F > \sigma_F$	No. of protein atoms	No. of atoms in sulfate groups	No. of IMP atoms	*R* factor	rms deviation in bond lengths	rms deviation in bond angles
C. Refinement parameters							
R-state GP*b*[a]	57,293	26,816	60	–	0.177	0.02 Å	4.0°
R-state PLPP-GP*b*-IMP	73,340	26,832	20	92	0.211	0.02 Å	4.1°

[a] From Barford and Johnson (1989).

[b] R_m is merging *R* defined as $R_m = \Sigma_h \Sigma_i |I(h) - I_i(h)| / \Sigma_h \Sigma_i I_i(h)$ where $I_i(h)$ and $I(h)$ are the *i*th and the mean measurement of the intensity of reflection *h*, respectively. The crystallographic *R* factor is defined as $R = \Sigma ||F_o| - |F_c|| / \Sigma |F_o|$ where F_o and F_c are the observed and the calculated structure factors, respectively.

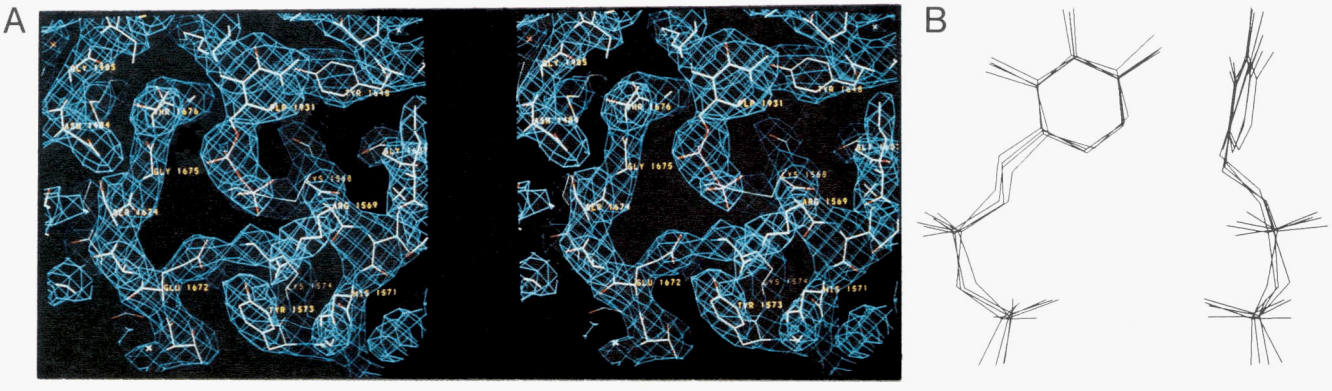

Fig. 1. **A**: Stereo diagram of electron density averaged over the four subunits in a map based on coefficients $2F_o - F_c$ and calculated phases after refinement. The map is contoured at 0.85 arbitrary units, which corresponds to about 1.3 the rms density. The unaveraged electron density is similar but the averaged density gives a clearer view. The diagram shows the modified cofactor PLPP and surrounding residues. (Residue numbers are increased by 1,000 to indicate subunit 1.) The side chains of Arg 569 and His 571 project out toward the viewer and that of Lys 568 is behind the two phosphates. The strong interaction between Lys 574 and Glu 672 is illustrated. Residues Gly 134 to Leu 136 are toward the viewer but have not been included in this view because they obscure the PLPP. **B**: Orthogonal views of the PLPP molecules from the four subunits superimposed.

GP*b* structure For example, in the PLPP structure, the *B* factors were 28 Å^2 for CB and increased along the side chain to 65 Å^2 for NE. In the native GP*b* structure the corresponding values were 20 Å^2 for CB with a slight increase to 30 Å^2 for NE. The results indicate that there is some additional flexibility in the arginine side chain in the PLPP structure but that only in subunit 2 is there a clear indication that it shifts its position so that there is a direct contact between the Arg 569 side chain and the second phosphate of PLPP. In the native R-state GP*b* structure there is a sulfate ion bound at the catalytic site. The initial difference map indicated that this sulfate had been displaced by the second phosphate of PLPP although the second phosphate position was distinct from that of the sulfate position. The displacement of the sulfate ion was confirmed by the refinement. At the Ser 14 phosphorylation site the electron density showed a strong isolated density indicating binding of a sulfate ion at the Ser-P site. At the allosteric nucleotide binding site, the binding of IMP resulted in displacement of the sulfate ion observed to be bound in native R-state GP*b* at the allosteric effector site.

Apart from the small adjustment of Arg 569 the overall structure of the PLPP–GP*b*–IMP complex is similar to the native R-state GP*b* structure (Kinemage 1). The rms differences in Cα coordinates for the four subunits are shown in Table 2. Those residues whose Cα atoms shifted more than 1.5 Å between PLPP–GP*b*–IMP and native R-state GP*b* correspond to 20–21, 209–212 (subunit 1 only), 253–262, 281, 313–318, 591–592 (subunit 4 only), and 830–832. These parts of the structure are the least well ordered in the R-state molecule, and the shifts in the coordinates reflect the uncertainty in the precise location of these more mobile parts of the structure. The mean rms difference in Cα coordinates for the four subunits between the PLPP and the native R-state structures is 0.57 Å and is similar to the value (0.59 Å) observed in the comparison of GP*b*–AMP complex with native R-state GP*b* structure (Barford et al., 1991). The average Cα atom temperature factors for the PLPP–GP*b*–IMP

Table 2. *Comparison of R-state GPb and R-state PLPP–GPb–IMP structures*

Subunit	rms deviation in Cα coordinates (Å)	Mean *B* factor (Å^2)		Torsion angles (°) for PLP and PLPP[a]					
		R-state GP*b*	R-state PLPP–GP*b*–IMP	R-state GP*b*		R-state PLPP–GP*b*–IMP			
				χ1	χ2	χ1	χ2	χ3	χ4
1	0.59	18	28	146	−81	177	−132	57	−80
2	0.62	19	29	−163	−151	−165	−144	19	−68
3	0.54	19	28	−113	169	−158	−98	−11	−61
4	0.51	23	32	177	−111	−163	−126	23	−73

[a] Definition of torsion angles: χ1, χ2, χ3, and χ4 refer to torsion angles about bonds in the sequence C5-C5′-OP4-P1-OP2-P2-OP5, where OP4 and OP2 are the phosphate ester oxygens.

structure are slightly greater than those observed for the native structure (Table 2) and are similar to those observed for the R-state GP*b*–AMP complex. (The three structures had been refined with similar protocols.) The AMP complex had been obtained by diffusion of nucleotide into preformed crystal, whereas in the PLPP-GP*b*–IMP complex the nucleotide had been present in the crystallization medium. Thus, in the present structure the increase in *B* factors is not a consequence of perturbation of the lattice on diffusion of ligand. The data in the PLPP-GP*b*–IMP complex had a better merging *R* factor than the native data (Table 1), indicating that the increase in *B* factors is not due to poorer data. The PLPP-GP*b*–IMP structure appears rather more mobile than the native R-state structure.

In the PLPP-GP*b*–IMP structure the position of the first phosphate group, P1, is similar to that observed for the 5′-phosphate of PLP in the native R-state GP*b* structure. The difference between the PLPP P1 position and the PLP phosphorus position is 0.7, 0.6, 0.5, and 0.3 Å for subunits 1, 2, 3, and 4, respectively. The temperature factors for the P2 atom ($B = 66$, 59, 66, 59 Å^2, respectively, for the four subunits) are higher than those observed for the P1 atom ($B = 21$, 23, 19, 26 Å^2, respectively) and indicate greater mobility for the second phosphate of the pyrophosphate moiety. The electron density shows essentially the same conformation for the pyrophosphate moiety of the PLPP in each of the four subunits (Fig. 1B), although there is some variation in the torsion angles (Table 2) that reflects the precision of the coordinates. (A difference in torsion angle of 10° results in a shift in position of the terminal atom by about 0.2 Å.) The $\chi 1$ values are similar to those for the native enzyme. We note that $\chi 2$ for PLP and $\chi 4$ for PLPP are not well defined at 2.8 Å resolution since it is difficult to distinguish the oxygen positions in the spherical electron density for the terminal phosphate groups, although some guidance is given by the contacts made to protein atoms. For the PLPP structure the near eclipsed conformation represented by $\chi 2$ directs the second phosphate, P2, toward the cluster of basic residues, Arg 569, Lys 574, and the main chain nitrogen of Gly 135, which form the substrate phosphate recognition site.

The contacts to the pyrophosphate moiety of PLPP are listed in Table 3 and illustrated in Figure 2 and Kinemage 1. As expected, the P1 phosphate makes similar contacts to those of the 5′ phosphate group of PLP in the native structure. In both the native and the PLPP R-state GP*b* structures, these include hydrogen bonds to the NZ group of Lys 568 and to the main chain nitrogens of Thr 676 and Gly 677 at the start of the $\alpha 21$ helix. There is some variation in the distances for the latter contacts in the different subunits that may reflect not only the limited precision at 2.8 Å resolution but also the lack of water in the refinement. In the T-state crystal structure, which was determined at 1.9 Å resolution, there are several well-located water molecules hydrogen-bonded to the cofactor phosphate (Oikonomakos et al., 1987). In the PLPP structure Lys 568 makes a contact to the bridging oxygen OP2. The second phosphate of PLPP makes a hydrogen bond from OP5 to the main chain nitrogen of Arg 569 and a short hydrogen bond from OP7 to Lys 574 NZ. In subunit 2 Arg 569 NH2 contacts the second phosphate at the OP6 position. In the other subunits this oxygen makes no hydrogen bonds, and although it is directed toward the main chain nitrogen of Gly 135, the separation is too long (over 3.9 Å) for a hydrogen bond. In the other subunits the closest approaches of the Arg 569 side chain (NE atom) to the P2 phosphate (OP7 atom) are 4.2, 4.9, and 4.7 Å for subunits 1, 3, and 4, respectively. In all of the four subunits Lys 568 makes an ionic link to Glu 672. Glu 672 is involved through its other carboxylate oxygen in a hydrogen-bond network that links Glu 672, Lys 574, Tyr 573, and Arg 569 (Fig. 2) (with the exception of subunit 2, where the link to Arg 569 is broken).

Comparison of the PLPP-GP*b*–IMP structure with the native T-state structure (after suitable transformation to superimpose the T-state structure onto the R-state structure) shows that if the modified cofactor were to be

Table 3. *Hydrogen bonds to phosphate oxygens in R-state PLPP-GPb–IMP complex*[a]

Atom	Subunit 1	Subunit 2	Subunit 3	Subunit 4
OP4	–	–	–	(Gly 677 N 3.9)
OP1	Lys 568 NZ 2.7	Lys 568 NZ 2.8	Lys 568 NZ 3.0	Lys 568 NZ 2.8
		Gly 677 N 3.1	(Gly 677 N 3.6)	
OP3	(Thr 676 N 3.7)	Thr 676 N 3.2	(Thr 676 N 3.4)	Thr 676 N 3.1
			Gly 677 N 2.7	Gly 677 N 2.9
OP2	Lys 568 NZ 2.7	Lys 568 NZ 2.8	Lys 568 NZ 2.9	Lys 568 NZ 2.7
OP5	Arg 569 N 2.5	Arg 569 N 3.1	Arg 569 N 3.3	(Arg 569 N 3.4)
OP6		Arg 569 NH2 2.5	–	–
OP7	Lys 574 NZ 2.7	Lys 574 NZ 2.6	Lys 574 NZ 2.5	Lys 574 NZ 2.5

[a] Hydrogen bond lengths are given in Å. Polar contacts <4 Å but too long for hydrogen bonds are shown in parentheses.

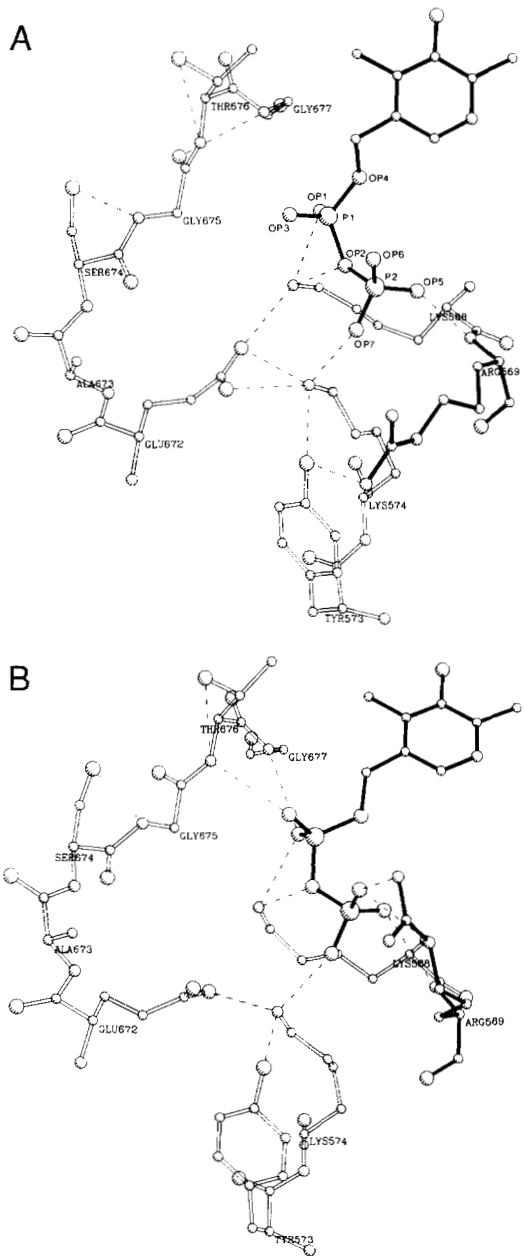

Fig. 2. Contacts to the pyrophosphate moiety of PLPP for (**A**) subunit 1 and (**B**) subunit 2. PLPP and Arg 569 are shown as solid lines. In subunit 2 Arg 569 has shifted from its position in native R-state GP*b* and makes a contact through its side chain to the second phosphate of PLPP.

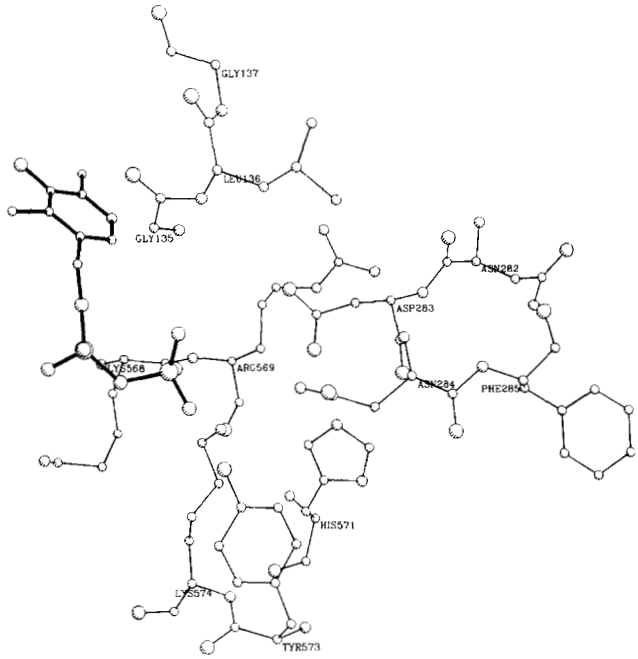

Fig. 3. PLPP from the R-state GP*b* structure with residues from T-state GP*b* (after superimposition on the R-state structure). The side chain of Asp 283 from the T-state structure is directed toward the second phosphate of PLPP. In the R state the loop residues 282–286 are displaced.

accommodated in the T-state structure, then the second phosphate would be directed toward the 280s loop and specifically toward Asp 283 and Asn 284 (Fig. 3; Kinemage 2). The closest approach of the P2 phosphate oxygen to the OD2 carboxylate oxygen of Asp 283 is 4 Å. Thus, comparison of T and R states suggests that were the PLPP-modified cofactor to be incorporated into the T-state structure, it would favor the displacement of the 280s loop through electrostatic repulsion between the second phosphate and Asp 283, but that the separation of these groups is that such a displacement like this may not be obligatory.

The position of the second phosphate in PLPP is distinct from the other anionic binding sites observed at the catalytic site. The P2 phosphorus position is 3 Å from the sulfur position of the sulfate ion that is noncovalently linked to the cofactor phosphate in R-state GP*b* crystals, and it is this sulfate ion that is displaced by the PLPP (Fig. 4; Kinemage 3). The complex of glucose-1-P with GP*b* has been studied in the R-state crystal form (Hu, 1991). In these experiments it was necessary to transfer the crystals from ammonium sulfate to sodium tartrate in order to displace the sulfate ion bound at the catalytic site and to allow binding of glucose-1-P. The sugar phosphate binds in a very similar conformation to that observed for glucose-1-P bound in the T state (Martin et al., 1990). In the R state the phosphate of glucose-1-P is in contact with Arg 569 but is not within hydrogen-bonding distance of the cofactor phosphate. The position of the P2 phosphate in the PLPP structure is 4.8 Å from the position observed for the phosphate of glucose-1-P. In the analysis of the T-state structure the most informative results concerning the mechanism were obtained with the small molecular weight substrate heptenitol and its conversion in the crystal to heptulose-2-phosphate (McLaughlin et al., 1984; Johnson et al., 1990). The structure of the heptulose-2-P complex with GP*b* in the T state was transformed to superimpose on the R-state structure. The po-

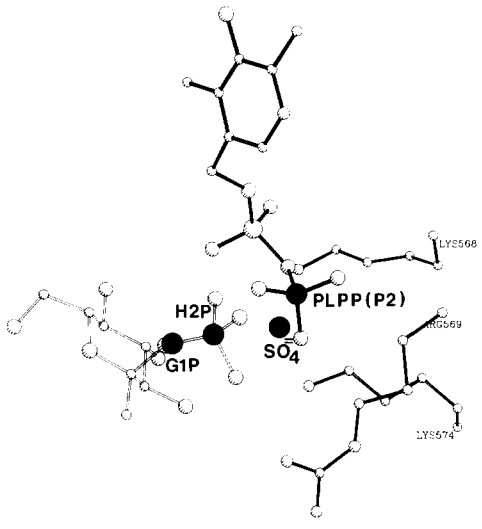

Fig. 4. Dianion binding sites at the catalytic site of GP*b*. The diagram shows the positions of PLPP (present work) and the positions of Lys 568, Arg 569, and Lys 574 as observed in R-state GP*b*. Sulfate (Barford & Johnson, 1989) and glucose-1-P (Hu, 1991) positions obtained from studies with the R-state crystals are shown as solid circles. Heptulose-2-P, obtained from studies with the T-state crystals (Johnson et al., 1990), is shown superimposed on the R-state structure.

sition of the P2 phosphorus in the PLPP structure is approximately 3 Å from the phosphate position of heptulose-2-P. Thus, the second phosphate site of PLPP is distinct from any of the other dianion binding sites observed in binding studies with T- or R-state crystal forms. Model building studies, in which the torsion angles for the pyrophosphate of PLPP were adjusted, show that it is possible to bring the P2 phosphate within 1.8 Å and 1 Å of the sulfur of the noncovalently bound sulfate and the phosphate of heptulose-2-phosphate, respectively, but that the covalent attachment of the second phosphate to the PLP in the PLPP structure does not allow it to reach the apparent substrate recognition sites. Likewise the noncovalent interactions prevent the sulfate ion or the phosphate of heptulose-2-phosphate reaching the P2 position observed for PLPP. Thus, it appears that a dianion can be accommodated in several different positions at the catalytic site within a sphere of about 5 Å in diameter. In each of these positions there are suitable stabilizing interactions with the enzyme and the precise location is dependent upon whether the dianion is covalently or noncovalently linked to other groups.

In the PLPP-GP*b*-IMP structure, IMP binds at the allosteric site, and the conformational changes observed at the cap′/α2 interface are almost identical to those observed when AMP is diffused into preformed R-state crystals (Barford et al., 1991). These changes include shifts in residues 42′ to 45′ of the cap′ loop so as to close the allosteric site, a shift of Tyr 75 so as to improve stacking between the base and the aromatic ring, and shifts in Arg 309 to allow contact between the arginine and the phosphate. The contacts made by IMP at the allosteric site are also essentially identical to those made by AMP when diffused into R-state crystals. The phosphate group is in a slightly different position to that observed for AMP and is close to the position occupied by a sulfate ion in the native R-state structure. The phosphate group of IMP is hydrogen-bonded to the side chain atoms of Tyr 75, Arg 309, and Arg 310 as in the AMP structure. The ribose is in the C3′ conformation and the O2′ hydroxyl is hydrogen-bonded to Asp 42′ of the other subunit at the monomer/dimer interface. The nucleotide base is stacked on one side against the aromatic ring of Tyr 75 and on the other side against the amide side chain of Asn 44′ and the peptide between 44′ and 45′ so that both amide groups are approximately coplanar with the nucleotide base. The side chain of Val 45′ is in van der Waals contact with the five-membered component of the purine ring and with the ribose. Previously (Barford et al., 1991) we noted that for AMP there is a hydrogen bond between the side chain of Asn 44′ and the N1 atom of the base in the R-state AMP complex and speculated that this interaction may serve to discriminate between AMP and IMP at the allosteric site and hence explain the difference in activation properties of these two nucleotides (Black & Wang, 1968). In the present IMP complex the position of Asn 44′ is close to that observed in the AMP complex but there is a slight tilt of the IMP base so that there is no hydrogen bond to the asparagine. The present results show that IMP can be accommodated at the R-state allosteric site with essentially the same geometry as AMP, and this suggests that Asn 44′ is unlikely to be a strong determinant in the discrimination against IMP.

In a recent publication on the R-state PLPP enzyme complexed with AMP and crystallized in an orthorhombic space group in the presence of polyethyleneglycol, Sprang et al. (1991) noted that there are hydrogen bonds from the main chain carbonyl oxygens of Ala 315 and Cys 318 to the N6 amino group of AMP and propose that these interactions favor AMP and discriminate against IMP binding at this site. In all four of the R-state structures crystallized in monoclinic space group from ammonium sulfate (the native R-state GP*b*, R-state GP*a*, R-state GP*b* complexed with AMP, and the present PLPP-GPb-IMP structure) the loop 315–321 is disordered, exhibits high temperature factors, and is not well supported by electron density. The position in which the loop has been placed by the refinement is too far away to make contacts with the nucleotide at the allosteric site. The refinement has also placed the side chain of Lys 315 in contact with N1 and O6 of IMP, but this position is not supported by electron density. It is not clear why this loop is disordered in the R-state crystal structures from ammonium sulfate. It is an exterior loop that connects an α helix (α8) to a strand of sheet and contains a reactive cysteine residue, Cys 318, that spectroscopic studies indicate is mobile (Griffiths et al., 1976). In the crystal structure, the loop is not involved in the dimer–tetramer contacts (Barford & Johnson, 1992) but is involved in a crystal lattice con-

tact for subunit 2. In the T-state structure this loop is also disordered and is involved in a lattice contact (Acharya et al., 1991). We note that in the present study IMP was cocrystallized with the enzyme, whereas in the AMP binding study AMP was diffused into preformed crystals. Cocrystallization in the presence of AMP leads to a doubling of the crystallographic c axis, indicating that there is some influence on the lattice contacts. This could be associated with ordering or shifts in the 315–321 loop, although we note that in the study with glucose-1-P where a similar doubling of the cell edge was observed there was no ordering of this loop. Crystallographic studies on the AMP cocrystallized complex are in progress. The notion that the 315–321 loop plays a role in the AMP binding is attractive and provides a more satisfactory explanation for the discrimination between IMP and AMP than the role invoked for Asn 44′. The result is also consistent with the spin label studies of Griffiths et al. (1976) in which Cys 318 was labeled with 4-(2-iodoacetamido)2,2,6,6-tetramethyl piperidinyloxyl. Addition of IMP to the spin-labeled enzyme resulted in a slight increase in the ESR ratio indicating an increase in the mobility of the label, whereas AMP resulted in a decrease of the ESR ratio indicating that the label is less mobile.

Discussion

Glycogen phosphorylase reconstituted with PLPP exhibits no enzyme activity. Solution studies had indicated that PLPP binds to apo-GP*b* in the same binding mode as PLP, and this is confirmed by the crystallographic results. Shimomura and Fukui (1978) observed that the rate of reconstitution of PLPP was 2,800 mol^{-1} s^{-1}, more than six times larger than that of PLP (420 mol^{-1} s^{-1}) from which it was inferred there is a stronger binding site for the diphosphate moiety. The crystallographic results show the extra phosphate can be accommodated within the catalytic site cavity and that it makes favorable contacts with the enzyme (three additional hydrogen bonds). Withers et al. (1982), on the basis of tertiary and quaternary structural information deduced from ^{31}P-NMR and ultracentrifugation data, showed that PLPP-GP*b* adopts a conformation that is more R-state-like than native GP*b*. Thus the binding of nucleotide AMPS is tighter (K_D = 40 μM) than to native GP*b* (K_D = 200 μM). Addition of AMP (or AMPS) resulted in complete conversion to a tetrameric form that could not be dissociated by glucose or caffeine. Glucose and caffeine are synergistic inhibitors that favor the T state and promote dissociation of tetramers to dimers with native GP*b*. These findings indicated that PLPP-GP*b* exists in a more activated R-state conformation than GP*b* in the absence of ligands, and that in the presence of the nucleotide activator the modified enzyme is locked into the activated conformation.

Previous crystallographic studies have shown the key conformational changes in the transition from T to R state (Barford & Johnson, 1989; Barford et al., 1991). At the catalytic site there is a displacement of an acidic residue (Asp 283) and its replacement by a basic group (Arg 569) and these changes contribute to the formation of a high affinity phosphate recognition site in the R state, and they also influence the state of ionization of the 5′-phosphate group of the cofactor. These tertiary structure changes are communicated to the subunit interface by displacement of the 280s loop (residues 282–286) and other shifts that are correlated with movements of the two antiparallel helices (the tower helices) of the subunit interface. The subsequent quaternary structure changes allow communication to the allosteric and Ser-P sites. The crystallographic results with PLPP-GP*b* show that the second phosphate can be accommodated in the R-state structure with essentially no conformational changes. However, if the modified cofactor were to be incorporated into the T-state structure of phosphorylase where the 280s loop is ordered, then there would be some electrostatic repulsion between the second phosphate and the side chain of Asp 283 (Fig. 3). This interaction would promote the displacement of the 280s loop from the catalytic site pocket and the concomitant shifts in the tower helices at the subunit interface and associated quaternary structure changes that characterize the T to R transition (Barford & Johnson, 1989; Barford et al., 1991). However, by itself the electrostatic repulsion from the groups separated by about 4 Å appears insufficient to make the displacement obligatory but only to encourage it, consistent with the results from solution studies.

The implications of the PLPP structure for the catalytic mechanism are less easy to assess from a single experiment. The results show that there are a number of positions that can be occupied by dianions at the catalytic site (i.e., the sites occupied by the second phosphate of PLPP, the sulfate ion, the phosphate of glucose-1-P and the phosphate of heptulose-2-P) and the question arises as to which sites, if any, are relevant for catalysis. The constellation of groups seen in the native GP*b* structure and the time-resolved studies on the formation of heptulose-2-P complex in the T-state crystals (Hajdu et al., 1987) provide support for a mechanism in which the attacking position for the substrate phosphate is located approximately 1 Å from the position observed in the product phosphate. In the natural reaction with glycogen substrates it was proposed that the cofactor phosphate promotes general acid attack by the substrate on the glucosyl polymer leading to cleavage of the glycosidic bond and formation of a carbonium ion intermediate (Fig. 5A). The reaction is completed by the attack of the substrate phosphate on the carbonium ion to give the product glucose-1-P. In this mechanism the phosphate shifts from a position in noncovalent contact with the substrate to a position in covalent contact as inferred from time-resolved studies on the conversion of heptenitol to heptulose-2-P (Hajdu et al., 1987), but in each of these positions it retains a hydrogen-bonding distance to the cofactor phosphate. The binding site observed for the sulfate ion is an

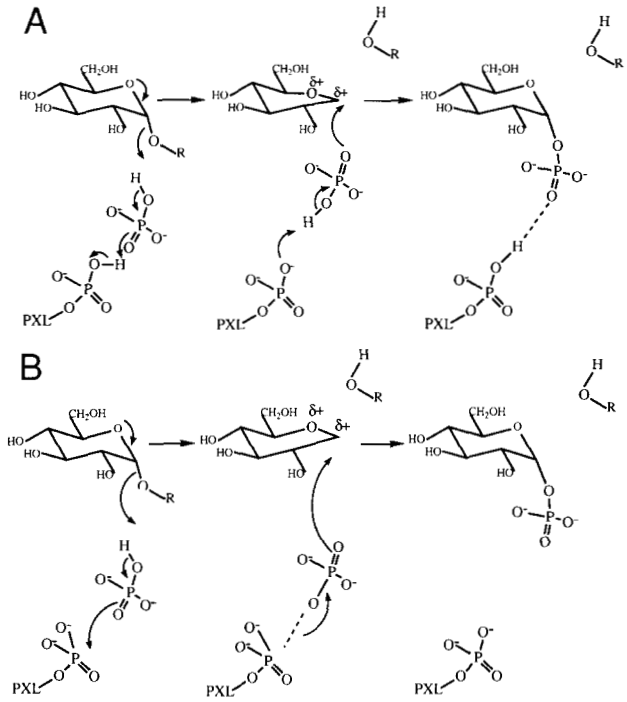

Fig. 5. Proposals for the catalytic mechanism. **A**: The PLP acts as a general acid-base to promote attack by the substrate phosphate. **B**: The PLP acts as an electrophile to withdraw electrons and promote attack by the substrate phosphate. For further details see text.

appropriate site for the attacking substrate phosphate (i.e., one of the sulfate oxygens is 2.3 and 3.6 Å from the positions for the α-1 oxygen and the C1 atom of heptulose-2-P, respectively), and the binding site for the phosphate of heptulose-2-P is an appropriate position for the product phosphate. The position for the phosphate observed in glucose-1-P complexes (Martin et al., 1990; Hu, 1991) most likely represents a nonproductive mode that can be altered by a simple rotation about the C1-O bond to the productive mode by the presence of the oligosaccharide substrate.

In the alternative proposal for the electrophilic mechanism, the cofactor phosphate acts as an electrophile to withdraw electrons from the substrate phosphate and destabilize the glycosidic bond (Fig. 5B) (Fukui et al., 1984; Madsen & Withers, 1986). A closer association between the cofactor and substrate phosphates is required than has been observed to date in the crystal structures, but such a close approach is mimicked by the PLPP analogue. If the position of the second phosphate of PLPP were to represent the position of the attacking phosphate, then one of the phosphate oxygens would be approximately 3.4 Å and 4.8 Å from the positions for the α-1 oxygen and the C1 carbon, respectively, of the glucosyl residue as defined by the positions of glucose-1-P and heptulose-2-P. These distances, although long, could be feasible for the catalytic mechanism. However, the present structure gives no evidence of additional strong interactions with the cofactor 5′-phosphate that have been invoked to provide stabilizing energy for the constrained dianion of the cofactor 5′-phosphate in this mechanism. The close approach of two phosphate groups in other enzymes such as the kinases is usually modulated by a metal ion. GP*b* reconstituted with PLPP-glucose in place of the natural cofactor results in a modified enzyme, which, in the presence of oligosaccharide, slowly releases glucose, incorporating it into the nonreducing group of oligosaccharide with the formation of the PLPP-GP*b* enzyme (Withers et al., 1981a; Takagi et al., 1982; Tagaya & Fukui, 1984). Crystallographic experiments are in progress to study the structure of the PLPP-glucose complex in the crystal, but the half life (approximately 2 days) makes this a difficult experiment for crystal growth of the reconstituted enzyme.

The results with the modified cofactor do not rule out the possibility that the second phosphate site represents the site of attack for the substrate phosphate as envisaged in the electrophilic mechanism, but the lack of additional factors to promote the proposed transition state-like constellation and the rather large distance to make a covalent bond to the glucose-1-P make this unlikely. The preferred interpretation of the structural results is that the second phosphate position of PLPP represents a fortuitous binding site that is determined by its covalent attachment to the cofactor phosphate and in which it is able to exploit interactions to nearby basic groups. The structural results indicate, however, that the second phosphate could rotate to a position nearer the substrate but this position is not observed in the crystal structure. The observations indicate the mobile nature of the dianion recognition site at the catalytic site that is consistent with the need for mobility of the phosphate group during catalysis.

Materials and methods

Rabbit muscle GP*b* was prepared (Fischer & Krebs, 1962) using 2-mercaptoethanol instead of cysteine and recrystallized at least four times. Bound nucleotides were removed (Melpidou & Oikonomakos, 1983). The enzyme concentration was determined from absorbance measurements at 280 nm (Kastenschmidt et al., 1968), and calculations of GP*b* molarity were based on a molecular weight of 97,434 for the monomeric subunit. GP*b* activity was determined at pH 6.8 and 30 °C in the direction of glycogen synthesis by measuring inorganic phosphate released (Leonidas et al., 1990). Initial velocities were calculated from the pseudo-first-order rate constants (Engers et al., 1970). Apoenzyme was prepared as described by Oikonomakos et al. (1987). Assays of the apoenzyme showed no activity, and the apoenzyme could be reconstituted with PLP to yield full activity (specific activity of 64 μmol/mg/min). GP*b* reconstituted with PLPP was prepared by incubating apoenzyme with 1.2-fold excess of PLPP in 50 mM β-glycerophosphate, 50 mM 2-mercaptoethanol, 1 mM EDTA buffer, pH 6.8 and 30 °C for 1 h. Unbound PLPP was removed by ammonium sulfate

precipitation (45%) of the protein derivative and dialysis first against 50 mM β-glycerophosphate, 50 mM 2-mercaptoethanol, 1 mM EDTA buffer, pH 6.8, and then against 10 mM β-glycerophosphate, 0.5 mM dithiothreitol, 0.5 mM EDTA, and 0.02% NaN_3 buffer, pH 7.5.

Crystals of R-state GP*b* reconstituted with PLPP were grown by the microdialysis method (Zeppezauer et al., 1968) from a concentration of 10 mg/mL in the presence of 1.2–1.4 M ammonium sulfate, 6 mM IMP in a buffer consisting of 10 mM β-glycerophosphate, 0.5 mM EDTA, 3 mM dithiothreitol, and 0.02% NaN_3, pH 7.5 at 16 °C. The crystals are monoclinic, $P2_1$ with unit cell dimensions a = 119.0 Å, b = 188.1 Å, c = 88.1 Å, β=109.3° with one tetramer MW 390,000 per asymmetric unit. In the PLPP-GP*b*-IMP crystals, the b dimension has decreased by 1% from the value, 190 Å, observed for the native GP*b* crystals (Barford & Johnson, 1989).

Three-dimensional data to 2.8 Å resolution were collected for the PLPP-GP*b*-IMP complex on an Arndt-Wonacott oscillation camera at the SERC Synchrotron Radiation Source at Daresbury, UK (Station 7.2) (Helliwell et al., 1982). The wavelength was 1.488 Å, and the synchrotron was operated at 2.0 GeV with current ranging from 250 to 150 mA. Six crystals were aligned with a* coincident with the crystal rotation axis and data recorded on contiguous packs with spindle oscillation range of 1° per film pack. A total of 90 packs (three films per pack) corresponding to a rotation range of 90° were recorded. The films were scanned with a 50-μm raster with an Optronics Microdensitometer. Crystal orientations were determined using STILLS (A.G.W. Leslie, P. Brick, & A.J. Wonacott, unpubl.) and REFIXNEW (Kabsch, 1988). Intensities were integrated with a modified version (D.I. Stuart et al., unpubl.) of MOSCO (Nybourg & Wonacott, 1977) implemented on a VAX 6210 computer. Standard corrections and subsequent scaling of the films were carried out with the CCP4 suite of programs. The overall merging R value for intensities of 107,286 reflections reduced to a unique set of 78,049 reflections was 0.108, and the mean fractional isomorphous difference between native R-state GP*b* and PLPP-GP*b*-IMP complex was 0.16 (Table 1).

The difference map between PLPP-GP*b*-IMP and native GP*b* (R state) showed additional electron density for the second phosphate attached to the PLP and for IMP bound at the allosteric site and displacement of sulfate ions from the catalytic and allosteric sites. There was no substantial conformational change. Coordinates for the additional phosphate group covalently linked to the cofactor and for IMP were added to the coordinate file with standard geometry.

The structure was refined using the program XPLOR (Brunger et al., 1987, 1989) for a tetramer of four equivalent subunits with the application of tight noncrystallographic restraints (200 kcal/mol), which serve to maintain equivalence of the subunits and increase the number of observations to parameters. The starting crystallographic R value was 0.378. Eight rounds of positional least-squares refinement were performed until the R factor converged. The noncrystallographic restraints were slowly reduced and finally released altogether. This was followed by a round of B-factor refinement and a final round of positional refinement. The final R value was 0.211 for all $F > \sigma_F$ comprising 73,340 reflections to 2.8 Å resolution. The rms deviation in bond lengths and bond angles were 0.02 Å and 4.1°, respectively. The mean difference in coordinates of the refined PLPP-GP*b*-IMP complex and the starting structure was 0.49 Å for main chain and 0.69 Å for side chain atoms. Water molecules were not included in the refinement at 2.8 Å resolution. Final refinement statistics are given in Table 1. After refinement the $2F_o - F_c$ electron density map was examined carefully for each of the four subunits, and with the exception of the Arg 569 side chain in subunit 2 the coordinates corresponded well to the observed electron density, indicating no need for further refinement. The coordinates have been deposited in the Protein Data Bank.

Protein coordinates and electron density maps were examined on an Evans and Sutherland PS390 with FRODO (Jones, 1978) modified by J.W. Pflugrath, M. Saper, R.E. Hubbard, and P.R. Evans. T-state structures were superimposed on R-state structure with the program ASH (Hendrickson, 1979).

PLPP was kindly provided by Professor T. Fukui. AMP, glucose-1-P (dipotassium salt), IMP, and ammonium sulfate were products of Sigma, and sodium β-glycerophosphate was obtained from Merck.

Acknowledgments

We thank Professor T. Fukui for his gift of PLPP, Dr. D.I. Stuart for his practical advice in the data processing, and H.S. Tsitoura for help in the data collection. We are grateful to the staff at the SERC's Synchrotron Radiation Source, Daresbury, UK. Financial support has been provided by the Daresbury Laboratory (under the minor grants scheme and the European Community Large Scale Facilities Programme) (N.G.O.) and EMBO (D.D.L.). L.N.J. is a member of the Oxford Centre for Molecular Sciences, which is supported by the SERC and the MRC.

References

Acharya, K.R., Stuart, D.I., Varvill, K.M., & Johnson, L.N. (1991). *Glycogen Phosphorylase: Description of the Protein Structure.* World Scientific, London.

Baranowski, T., Illingworth, B., Brown, O.H., & Cori, C.F. (1957). The isolation of pyridoxal 5'-phosphate from crystalline muscle phosphorylase. *Biochim. Biophys. Acta 25,* 16–21.

Barford, D., Hu, S.-H., & Johnson, L.N. (1991). Structural mechanism for glycogen phosphorylase control by phosphorylation and AMP. *J. Mol. Biol. 218,* 233–260.

Barford, D. & Johnson, L.N. (1989). The allosteric transition of glycogen phosphorylase. *Nature 340,* 609–614.

Barford, D. & Johnson, L.N. (1992). The molecular mechanism for the tetrameric association of glycogen phosphorylase promoted by protein phosphorylation. *Protein Sci. 1,* 472–493.

Black, W.J. & Wang, J.H. (1968). Studies on the allosteric activation of glycogen phosphorylase *b* by nucleotides. *J. Biol. Chem. 243,* 5892–5898.

Brunger, A.T., Karplus, M., & Petsko, G.A. (1989). Crystallographic

refinement by simulated annealing: Application to crambin. *Acta Crystallogr. A45*, 50-61.
Brunger, A.T., Kuriyan, J., & Karplus, M. (1987). Crystallographic R factor refinement by molecular dynamics. *Science 235*, 458-460.
Engers, H.D., Shechosky, S., & Madsen, N.B. (1970). Kinetic mechanism of phosphorylase a. *Can. J. Biochem. 48*, 746-754.
Feldman, K. & Hull, W.E. (1977). ^{31}P nuclear magnetic resonance studies of glycogen phosphorylase from rabbit muscle: Ionisation states of pyridoxal 5'-phosphate. *Proc. Natl. Acad. Sci. USA 74*, 856-860.
Fischer, E.H., Kent, A.B., Snyder, E.R., & Krebs, E.G. (1958). Reaction of sodium borohydride with rabbit muscle phosphorylase. *J. Am. Chem. Soc. 80*, 2906-2907
Fischer, E.H. & Krebs, E.G. (1962). Muscle phosphorylase b. *Methods Enzymol. 5*, 369-372.
Fukui, T., Tagaya, M., Tagaki, M., & Shimomura, S. (1984). Role of pyridoxal 5'-phosphate in the catalytic mechanism of glycogen phosphorylase. In *Chemical and Biological Aspects of Vitamin B6 Catalysis* (Evangelopoulos, A.E., Ed.), Part A, pp. 161-170. Alan R. Liss, New York.
Graves, D.J. & Wang, J.H. (1972). α-Glucan phosphorylases-Chemical and physical basis of catalysis and control. In *The Enzymes*, 3rd Ed. (Boyer, P.D., Ed.), Vol. 7, pp. 435-482. Academic Press, New York.
Griffiths, J.R., Dwek, R.A., & Radda, G.K. (1976). Conformational change in glycogen phosphorylase studied with a spin label probe. *Eur. J. Biochem. 61*, 237-242.
Hajdu, J., Acharya, K.R., Stuart, D.I., McLaughlin, P.J., Barford, D., Oikonomakos, N.G., Klein, H., & Johnson, L.N. (1987). Catalysis in the crystal: Synchrotron radiation studies with glycogen phosphorylase b. *EMBO J. 6*, 539-546.
Hedrick, J.L., Shaltiel, S., & Fischer, E.H. (1966). On the role of pyridoxal 5'-phosphate in phosphorylase. III. Physicochemical properties and reconstitution of apophosphorylase b. *Biochemistry 5*, 2117-2125.
Helliwell, J.R., Greenhough, T.J., Carr, P.D., Rule, S.A., Moore, P.R., Thompson, A.W., & Worgan, J.S. (1982). A central data collection facility for protein crystallography, small angle diffraction and scattering with the Daresbury Laboratory synchrotron radiation source. *J. Phys. E 15*, 1363-1372.
Helmreich, E.J.M. & Klein, H. (1980). The role of pyridoxal phosphate in the catalysis of glycogen phosphorylases. *Angew. Chem. Int. Ed. Engl. 19*, 441-455.
Hendrickson, W.A. (1979). Transformations to optimise the superposition of similar structures. *Acta Crystallogr. A35*, 158-173.
Hu, S.-H. (1991). Crystallographic studies on activated glycogen phosphorylase. Ph.D. Thesis, University of Oxford.
Johnson, L.N., Acharya, K.R., Jordan, M.D., & McLaughlin, P.J. (1990). Refined crystal structure of the phosphorylase heptulose-2-phosphate oligosaccharide-AMP complex. *J. Mol. Biol. 211*, 645-661.
Johnson, L.N., Hajdu, J., Acharya, K.R., Stuart, D.I., McLaughlin, P.J., Oikonomakos, N.G., & Barford, D. (1989). Glycogen phosphorylase. In *Allosteric Enzymes* (G. Herve, Ed.), pp. 81-127. CRC Press, Boca Raton, Florida.
Jones, A.T. (1978). A graphics model building and refinement system for macromolecules. *J. Appl. Crystallogr. 11*, 268-272.
Kabsch, W.J. (1988). Evaluation of single crystal X-ray diffraction data for a position sensitive detector. *J. Appl. Crystallogr. 21*, 916-924.
Kastenschmidt, L.L., Kastenschmidt, J., & Helmreich, E. (1968). The effect of temperature on the allosteric transition of glycogen phosphorylase b. *Biochemistry 7*, 3590-3608.
Klein, H., Im, M.-J., & Palm, D. (1986). The role of pyridoxal 5'-phosphate and orthophosphate in general acid-base catalysis by α-glucan phosphorylases. *Eur. J. Biochem. 157*, 107-114.
Leonidas, D.D., Oikonomakos, N.G., & Papageorgiou, A.C. (1991). Sulphate activates phosphorylase *b* by binding to the Ser-P site. *Biochim. Biophys. Acta 1076*, 305-307.
Leonidas, D.D., Oikonomakos, N.G., Papageorgiou, A.C., Xenakis, A., Cazianis, C.T., & Bem, F. (1990). The ammonium sulphate activation of phosphorylase *b*. *FEBS Lett. 261*, 23-27.
Madsen, N.B. (1986). Glycogen phosphorylase: control by phosphorylation. In *The Enzymes*, 3rd Ed. (Boyer, P.D. & Krebs, E.G. Eds.), Vol. 17, pp. 366-394. Academic Press, New York.
Madsen, N.B. & Withers, S.G. (1986). Glycogen phosphorylase. In *Coenzymes and Cofactors*, Vol. 1. *Vitamin B6 Pyridoxal Phosphate* (Dolphin, D., Poulson, R., & Avramovic, O., Eds.), pp. 355-389. John Wiley, New York.
Martin, J.L., Johnson, L.N., & Withers, S.G. (1990). Comparison of the binding of glucose and glucose-1-phosphate derivatives to T state glycogen phosphorylase *b*. *Biochemistry 29*, 10745-10757.
McLaughlin, P.J., Stuart, D.I., Klein, H.W., Oikonomakos, N.G., & Johnson, L.N. (1984). Substrate cofactor interactions for glycogen phosphorylase b: A binding study in the crystal for heptenitol and heptulose-2-phosphate. *Biochemistry 23*, 5862-5873.
Melpidou, A.E. & Oikonomakos, N.G. (1983). Effects of glucose-6-P on the catalytic and structural properties of glycogen phosphorylase a. *FEBS Lett. 154*, 105-110.
Nybourg, J. & Wonacott, A.J. (1977). Computer programmes. In *The Rotation Method in Crystallography* (Arndt, U.W. & Wonacott, A.J., Eds.), pp. 139-152. North-Holland, Amsterdam.
Oikonomakos, N.G., Acharya, K.R., & Johnson, L.N. (1991). Rabbit muscle glycogen phosphorylase b: Structural basis of activation and catalysis. In *Post-Translational Control of Proteins* (Crabbe, J.C. & Harding, T., Eds.), pp. 81-151. CRC Press, Boca Raton, Florida.
Oikonomakos, N.G., Johnson, L.N., Acharya, K.R., Stuart, D.I., Barford, D., Hajdu, J., Varvill, K.M., Melpidou, A.E., Papageorgiou, T., Graves, D.J., & Palm, D. (1987). Pyridoxal phosphate site in glycogen phosphorylase b: Structure in native enzyme and in three derivatives with modified cofactors. *Biochemistry 26*, 8381-8389.
Palm, D., Klein, H.W., Schinzel, R., Buehner, M., & Helmreich, E.J.M. (1990). The role of pyridoxal 5'-phosphate in glycogen phosphorylase catalysis. *Biochemistry 29*, 1099-1107.
Parrish, R.F., Uhing, R.J., & Graves, D.J. (1977). Effect of phosphate analogues on the activity of pyridoxal reconstituted glycogen phosphorylase. *Biochemistry 16*, 4824-4831.
Perutz, M.F. (1970). Stereochemistry of cooperative effects in hemoglobin. *Nature 228*, 726-734.
Shaltiel, S., Hedrick, J.L., Pocker, A., & Fischer, E.H. (1969). Reconstitution of apophosphorylase with pyridoxal 5-phosphate analogues. *Biochemistry 8*, 5189-5196.
Shimomura, S. & Fukui, T. (1978). Characterisation of the pyridoxal phosphate site in glycogen phosphorylase b from rabbit muscle. *Biochemistry 17*, 5359-5367.
Sprang, S.R., Acharya, K.R., Goldsmith, E.J., Stuart, D.I., Varvill, K., Fletterick, R.J., Madsen, N.B., & Johnson, L.N. (1988). Structural changes in glycogen phosphorylase induced by phosphorylation. *Nature 336*, 215-221.
Sprang, S.R., Madsen, N.B., & Withers, S.G. (1992). Multiple phosphate positions in the catalytic site of glycogen phosphorylase: Structure of the pyridoxal-5'-pyrophosphate coenzyme-substrate analog. *Protein Sci. 1*, 1100-1111.
Sprang, S.R., Withers, S.G., Goldsmith, E.J., Fletterick, R.J., & Madsen, N.B. (1991). The structural basis for the association of glycogen phosphorylases b by AMP. *Science 254*, 1367-1371.
Tagaya, M. & Fukui, T. (1984). Catalytic reaction of glycogen phosphorylase reconstituted with a coenzyme substrate conjugate. *J. Biol. Chem. 259*, 4860-4865.
Takagi, M., Fukui, T., & Shimomura, S. (1982). Catalytic mechanism of glycogen phosphorylase; pyridoxal-5'-diphospho-1-α-D-glucose as a transition state analogue. *Proc. Natl. Acad. Sci. USA 79*, 3716-3719.
Titani, K., Koide, A., Herman, J., Ericson, L.H., Kumar, S., Wade, R.D., Walsh, K.A, Neurath, H., & Fischer, E.H. (1977). Complete amino acid sequence of rabbit muscle glycogen phosphorylase. *Proc. Natl. Acad. Sci. USA 74*, 4762-4766.
Withers, S.G., Madsen, N.B., & Sykes, B.D. (1981a). Active form of pyridoxal phosphate in glycogen phosphorylase. Phosphate-31 nuclear magnetic resonance investigation. *Biochemistry 20*, 1748-1756.
Withers, S.G., Madsen, N.B., & Sykes, B.D. (1982). Covalently activated glycogen phosphorylase: A phosphorus-31 nuclear magnetic resonance and ultracentrifugation analysis. *Biochemistry 21*, 6716-6722.
Withers, S.G., Madsen, N.B., Sykes, B.D., Takagi, M., Shimomura, S., & Fukui, T. (1981b). Evidence for direct phosphate-phosphate interaction between pyridoxal phosphate and substrate in the glycogen phosphorylase catalytic mechanism. *J. Biol. Chem. 256*, 10759-10762.
Zeppezauer, M., Edlund, H., & Zeppezauer, E.S. (1968). A microdialysis method for protein crystallisation. *Arch. Biochem. Biophys. 126*, 564-574.